Systemic Ghrelin Treatment Induces Rapid, Transient, and Asymmetric Changes in the Metabolic Activity of the Mouse Brain

Pablo Nicolás de Francesco, Gimena Fernandez, Maia Uriarte, Leandro Urrutia, Magdalena Ponce de León, Jean-Alain Fehrentz, German Falasco, Mario Perello

Systemic ghrelin treatment induces rapid, transient and asymmetric changes in the metabolic activity of the mouse brain

Pablo Nicolás De Francesco[1], Gimena Fernandez[1], Maia Uriarte[1], Leandro Urrutia[2], Magdalena Ponce de León[2], Jean-Alain Fehrentz[3], German Falasco[2], Mario Perello[1,4]

[1]Laboratory of Neurophysiology of the Multidisciplinary Institute of Cell Biology [IMBICE, Argentine Research Council (CONICET) and Scientific Research Commission, Province of Buenos Aires (CIC-PBA), National University of La Plata], La Plata, Buenos Aires, Argentina.

[2]Center of Molecular Imaging of Neurological Research Institute (FLENI), Escobar, Buenos Aires, Argentina

[3]Institut des Biomolécules Max Mousseron-UMR5247, Pôle Chimie Balard Recherche, Montpellier, France.

[4]Department of Surgical Sciences, Functional Pharmacology and Neuroscience, University of Uppsala, Uppsala, Sweden.

Short title: Brain areas responsive to ghrelin treatment.

Corresponding Author:
Dr. Mario Perelló
Laboratory of Neurophysiology, Multidisciplinary Institute of Cell Biology
Calle 526 S/N entre 10 y 11. La Plata, Buenos Aires, 1900, Argentina
Tel: +54 9 221 4210112. Email: mperello@imbice.gov.ar

Keywords: ^{18}F-fluoro-2-deoxyglucose, GHSR, central nervous system, circumventricular organs.

ABSTRACT

Introduction: Ghrelin regulates a variety of functions by acting in the brain. The targets of ghrelin in the mouse brain have been mainly mapped using immunolabeling against c-Fos, a transcription factor used as a marker of cellular activation, but such analysis has several limitations. Here, we used positron emission tomography in mice to investigate the brain areas responsive to ghrelin. Methods: We analyzed in male mice the brain areas responsive to systemically-injected ghrelin using positron emission tomography imaging of ^{18}F-fluoro-2-deoxyglucose (^{18}F-FDG) uptake, an indicator of metabolic rate. Additionally, we studied if systemic administration of fluorescent-ghrelin or native ghrelin display symmetric accessibility or induction of c-Fos, respectively, in the brain of male mice. Results: Ghrelin increased ^{18}F-FDG uptake in few specific areas of the isocortex, striatum, pallidum, thalamus and midbrain at 0-10-min post-treatment. At the 10-20- and 20-30-min post-treatment, ghrelin induced mixed changes in ^{18}F-FDG uptake in specific areas of isocortex, striatum, pallidum, thalamus and midbrain, as well as in areas of the olfactory areas, hippocampal and retrohippocampal regions, hypothalamus, pons, medulla and even the cerebellum. Ghrelin-induced changes in ^{18}F-FDG uptake were transient and asymmetric. Systemically-administrated fluorescent-ghrelin labeled midline brain areas known to contain fenestrated capillaries and the hypothalamic arcuate nucleus, where a symmetric labeling was observed. Ghrelin treatment also induced a symmetric increased c-Fos labeling in the arcuate nucleus. Discussion/Conclusion: Systemically-injected ghrelin transiently and asymmetrically affects the metabolic activity of the brain of male mice in a wide range of areas, in a food intake independent manner. The neurobiological bases of such asymmetry seem to be independent of the accessibility of ghrelin into the brain.

INTRODUCTION

Ghrelin is a stomach-derived peptide hormone [1]. Plasma ghrelin levels increase before meals, decline after meals, and then increase gradually until the next preprandial period [2]. Plasma ghrelin levels also increase in energy deficit conditions, such as fasting, malnutrition, anorexia nervosa or cachexia, among others [3–6]. Ghrelin acts via the growth hormone secretagogue receptor (GHSR) [1], which is highly expressed in some brain areas and in the pituitary [7,8]. It is widely recognized that ghrelin treatment displays a variety of neuroendocrine, autonomic, metabolic and behavioral effects in humans and rodents. Ghrelin increases plasma levels of growth hormone as well as prolactin, adrenocorticotropic hormone and glucocorticoid [9–15]. The ghrelin-induced activation of these neuroendocrine axes together with the putative action of ghrelin on other organs, such as pancreas, promotes an increase of glycaemia [16]. Ghrelin administration also potently increases food intake and modulates rewarding aspects of appetite [17]. In addition, ghrelin modulates the activity of the autonomic nervous system and consequently increases gastric emptying and decreases blood pressure [18–20]. Preclinical studies in rodents have shown that ghrelin also influences learning and memory, but the extent to which ghrelin affects these cognitive functions in humans is currently uncertain [21,22]. Thus, ghrelin treatment displays pleiotropic central actions, some of which may have important clinical implications. However, the brain areas that sense, integrate and execute ghrelin signaling are only poorly known.

In mice and rats, GHSR is expressed in a variety of brain areas that could directly mediate the effects of ghrelin. Strikingly, however, studies using fluorescent analogs of ghrelin in mice have shown that the accessibility of plasma ghrelin is restricted to few brain areas [23–25]. In particular, systemically-injected fluorescent ghrelin diffuses into the median eminence (ME) and into the neighbor ventromedial region of the hypothalamic arcuate nucleus (ARH), which contains fenestrated capillaries of the hypophyseal portal system [23,26,27]. Systemically-injected fluorescent ghrelin also diffuses through fenestrated capillaries into the area postrema (AP) [28]. In mice, ghrelin does not seem to cross the blood-brain-barrier from the blood to the brain [29], but it can be transported towards the cerebrospinal fluid through the blood-cerebrospinal fluid barrier [30,31]. From the cerebrospinal fluid, ghrelin can target some periventricular brain areas, such as some hypothalamic nuclei [30,32]. The neuronal targets of ghrelin has been extensively mapped by assessing the induction of the immediate early gene *c-fos*, and it has been mainly reported that systemically-injected ghrelin mainly increases c-Fos levels in the ARH of mice

and rats [23,28,33–37], whereas it does not increase c-Fos levels in some areas known to express GHSR and that could mediate well-established effects of ghrelin [38]. These observations also suggest that the accessibility of plasma ghrelin to the mouse brain is limited. Nevertheless, the capability of c-Fos induction to faithfully estimate the brain areas responsive to ghrelin has important limitations. For instance, c-Fos induction may occur in neurons that are indirect targets of ghrelin. Also, *c-fos* reflects an up-regulation of some signal transduction pathways, which may be dissociated from electrical neuronal activity [39]. In addition, c-Fos does not provide information regarding neurons that are inhibited by ghrelin. Thus, the use of alternative approaches is important to complement c-Fos mapping studies and gain further insights of the central targets of ghrelin.

Here, we used positron emission tomography (PET) to assess the ^{18}F-2-deoxyglucose (FDG) uptake and estimate the changes in the metabolic activity induced by ghrelin treatment in the mouse brain. In order to maximize the chances to unmask putative effects of ghrelin on the metabolic activity of the brain, the current study was performed in male mice, which have been shown to be significantly more responsive to the orexigenic and GH secretagogue effects of ghrelin than female mice [40]. Since we found that ghrelin induces asymmetric changes in metabolic activity of the brain of male mice, we studied if systemically-administrated fluorescent-ghrelin displayed symmetric brain accessibility as well as if ghrelin treatment produced symmetric induction of c-Fos in the ARH.

MATERIALS AND METHODS

1. Mice. Adult (8-12 weeks old) male C57BL/6 wild-type mice were generated in the animal facility of the IMBICE. A set of 26 mice was shipped to the animal facility of the FLENI to perform the PET studies. In both animal facilities, mice were housed in a 12-h light/dark cycle with regular chow and water available *ad libitum*. In all cases, mice were individually housed three days before the experiments, which were performed between 9 a.m. and 12 a.m. in all cases. This study was carried out in strict accordance with the recommendations in the Guide for the Care and Use of Laboratory Animals of the National Institutes of Health, and all efforts were made to minimize suffering. All experimentation received approval from the Institutional Animal Care and Use Committees located in the Multidisciplinary Institute of Cell Biology (approval ID 17-0221).

2. Ghrelin variants. Ghrelin (GSS(octanoyl)FLSPEHQKAQQRKESKKPPAKLQPR) was purchased from Global Peptide (cat# PI-G-03). Fr-ghrelin [GSD(octanoyl)FLSPEHQRVQQRKESC-(DY-647P)] is a variant of ghrelin conjugated to DY-647P fluorophore through a C-terminal Cys. Fr-ghrelin was synthesized by linking DY-647P-maleimide to a 19-residues ghrelin analog that contains the initial 18 residues of the ghrelin sequence, but replacing the serine in position 3 by aspartic acid whose side-chain was amidated with octylamine, and containing a cysteine at the position 19. Fr-ghrelin was synthesized, purified by high-performance liquid chromatography and characterized by mass spectrometry, as we have done in the past [41]. Fr-ghrelin was previously validated and shown to increase food intake *in vivo* and label GHSR-expressing brain areas in wild-type mice but not in GHSR-deficient mice [31].

3. Assessment of ^{18}F-FDG uptake in the mouse brain in response to ghrelin treatment and spatial quantification. Here, PET data was acquired two times per mouse, after ghrelin and vehicle treatments over different days, in a randomized crossover design. In the morning, mice were subcutaneously injected with ghrelin (0.06 nmol/g BW) or vehicle and intraperitoneally injected with ^{18}F-FDG (25 µCi/gr), with a variable time difference (-10 min, 0 min and +10 min) between both injections, as shown in Fig. 1. These PET studies, hereafter named E1, E2 and E3, were designed to assess ^{18}F-FDG uptake in the 0–10, 10–20 or 20–30 minutes time windows after ghrelin treatment, and had 10, 6 and 10 mice, respectively. The tested dose of ghrelin induces a transient ~50-fold increase in the plasma ghrelin levels, similar to the one observed in 5-day calorie-restricted mice [42], which return

to basal levels at ~45-min after treatment [23]. Before treatments, food pellets were removed from the home cages. After treatments, anesthesia was induced by inhalation of isoflurane (4.5% for induction and 1.5% for maintenance) supplemented with oxygen for approximately 2-3 min. PET data was acquired during 12 minutes per mouse using list-mode acquisition.

Images were acquired with a preclinical PET TriFoil Lab-PET 4, with an approximated spatial resolution of 1.2 mm full width at half maximum (FWHM) and an imaging field of view (FOV) of 3.7 cm axial and 11 cm trans-axial. Images were reconstructed using an OSEM 3D algorithm with 30 iterations to maximize the signal-to-noise ratio. If motion was detected during acquisition, a realign algorithm was applied to the temporal dynamic reconstruction using SPM12 on MATLAB. For image spatial processing, brain images were normalized to a previously generated normal C57BL/6 wild-type mice ^{18}F-FDG template, using Advanced Normalization Tools registration pipeline comprising SyN (image registration). Smoothing using an Isotropic Gaussian kernel with three times the voxel size (0.75x0.75x1.791mm) FWHM was made with SPM12 on MATLAB. ^{18}F-FDG uptake was intensity normalized to gray cerebellum mean based on the Allen Reference Atlas. A Harderian Glands mask was not applied since they do not affect registration pipeline. Statistical comparisons of the ^{18}F-FDG uptake between conditions were performed for each experiment as described in sub-section 6.

The distribution of areas with significant changes in ^{18}F-FDG uptake was assessed in regions from the Allen Reference Atlas ontology tree (at 50 μm resolution) using python scripts and the Allen Reference Space SDK [43]. The analysis was performed only on grey matter regions, excluding those with less than 2000 voxels (bilateral, equivalent to 0.25 mm^3). The tree was collapsed from bottom to top until all terminal nodes met this requirement, and less than 10% of the volume was excluded in any terminal branch. The cortical areas and the superior colliculi had their layer nodes collapsed regardless of their size. This process resulted in 170 terminal nodes, from which hemilateral masks where created. Within each region, we determined the number voxels that were significantly activated or inhibited, and set a minimum threshold of 300 voxels (per side) to produce a list of responding hemilateral regions for each experiment.

4. Visualization of brain areas accessible to systemically-injected Fr-ghrelin. An independent set of mice was subcutaneously injected with vehicle alone (n=5) or containing Fr-ghrelin (1.2 nmol/g BW, n=6). Before treatments, food pellets were removed from the

home cages. This dose of Fr-ghrelin is the minimal dose that allows the direct visualization of Fr-ghrelin in the fixed brain (unpublished observations). Fifteen minutes after treatment, mice were anesthetized and perfused with formalin. Brains were extracted, post-fixed, immersed in 20% sucrose, and frozen. Next, a shallow longitudinal incision down the right hemisphere was made in order to track the laterality of the sections, and brains were coronally cut at 40 µm into four equal series on a cryostat. Brain sections were sequentially mounted on glass slides, coverslipped with mounting medium containing Hoechst. Fluorescent images of the brain sections were acquired using structured illumination in a Zeiss Axio Observer D1 fluorescence microscope equipped with an Apotome.2 module and an AxioCam 506 monochrome camera. The presence of Fr-ghrelin signal was determined in 1-in-4 series from the level of the olfactory bulbs down to the cervical spinal cord. Fluorescent images were acquired with a 10x/0.45 objective, using an automated tiling strategy to image all the brain sections. Also, higher magnification images of selected regions were acquired using a 40x/0.95 objective. Tiles from each mouse were aligned for neuroanatomical analysis using the Fiji plugin TrackEM2 [44,45]. The Allen mouse brain atlas was used to identify brain sections and to describe the brain nuclei. Estimates of Fr-ghrelin signal for the different brain regions were made by considering both signal strength and number of labeled cells as compared to the signal observed in samples from vehicle-treated mice. Fr-ghrelin signal was quantified as mean fluorescent intensity and expressed in arbitrary units (A.U.)

5. Assessment of ghrelin-induced c-Fos in the mouse brain. Another set of mice was subcutaneously injected with vehicle alone (n=5) or containing ghrelin (0.06 nmol/g BW, n=5) between 8:00 and 10:00 a.m. Before treatments, food pellets were removed from the home cages. Two hours after treatment, mice were anesthetized and perfused with formalin. Brains of perfused mice were removed, post-fixed, immersed in 20% sucrose and frozen. As described above, a shallow longitudinal incision down the right hemisphere was made in order to track the laterality of the sections, and brains were coronally cut at 40 µm into three equal series on a cryostat. C-Fos immunostaining was also performed as described. Briefly, sections were pretreated with 0.5% H_2O_2, treated with blocking solution (3% normal donkey serum and 0.25% TritonX in PBS) and incubated with anti-c-Fos antibody (Calbiochem/Oncogene, cat# PC38, 1:20.000) for two days at 4°C. Then, sections were treated with biotinylated donkey anti-rabbit antibody (Jackson ImmunoResearch Laboratories, West Grove, PA, 1:3.000) for 1 h and with Vectastain Elite ABC kit (Vector Laboratories, cat # PK6200) for 1 h, according to manufacturer's protocols. A visible signal

was developed with 3-3'-diaminobenzidine (DAB)/Nickel solution, giving a black/purple precipitate. Sections were sequentially mounted on glass slides and coverslipped with mounting media. Bright-field images were acquired with a Nikon Eclipse 50i and a DS-Ri1 Nikon digital camera. The number of c-Fos-immunoreactive (IR) cells in the right and left ARH were estimated in coronal brain sections between bregma -1.58 and -1.94 mm. Anatomical limits of the ARH were identified using a mouse brain atlas [46]. Cells containing a distinct nuclear black/purple precipitate were quantified in one out of three complete series of coronal sections through the whole ARH. Blind quantitative analysis was performed independently by two observers and expressed as c-Fos-IR cells per coronal section per side.

6. Statistical analysis. Statistical analysis of the PET signal was performed using SPM12 on MATLAB. For each experiment, statistical comparisons of the ^{18}F-FDG uptake between ghrelin and vehicle condition were performed using paired Student's t test. A p-value less than 0.05 was considered significant. Using a general linear model, a contrast of parameter estimates was calculated for each experiment. In order to have an accurate anatomical reference, all results of statistical differences were co-registered with the serial two photon tomography average template (50 µm resolution version) from the Allen mouse Common Coordinate Framework (CCFv3) Reference Atlas [47].

Statistical analyses of Fr-ghrelin signal and c-Fos levels were performed using GraphPad Prism 6.0 and differences were considered significant when $P<0.05$. An unpaired t-test was used to compared mean fluorescent intensity or the number of c-Fos-IR cells per section in the ARC of vehicle treated mice vs ghrelin- or Fr-ghrelin-treated mice, respectively. A paired t-test analysis was used to compare mean fluorescent intensity or the number of c-Fos-IR cells per section per side of the right and left ARH of ghrelin- and Fr-ghrelin-treated mice, respectively.

RESULTS

Systemically injected ghrelin induces rapid, transient and asymmetric changes in the ^{18}F-FDG uptake. The effects of ghrelin on brain glucose metabolism were estimated based on the PET analysis of ^{18}F-FDG uptake. The observed differences in ^{18}F-FDG uptake are shown in Fig. 2-4 and outlined in Fig. 5.

In the ~0-10 min post-treatment time window, ghrelin increased ^{18}F-FDG uptake in in a small set of specific brain areas. In the cerebral cortex, ^{18}F-FDG uptake increased in the right secondary motor area. Within the cerebral nuclei, ^{18}F-FDG uptake increased in the right caudoputamen of the dorsal region of the striatum, in the right ventral part of the lateral septal nucleus, and in the right bed nuclei of the stria terminalis of the caudal pallidum. Within the thalamus, ^{18}F-FDG uptake increased in the right sensory-motor cortex related areas, in the right intralaminar nuclei of the dorsal thalamus and in the left side of medial group of the dorsal thalamus. Also, ^{18}F-FDG uptake increased in the right motor-related area of the superior colliculus in the midbrain.

In the ~10-20 min post-treatment time window, ghrelin treatment increased and decreased ^{18}F-FDG uptake in specific brain areas. In the isocortex, ^{18}F-FDG uptake decreased in the both sides of the primary and secondary motor areas, of the prelimbic and infralimbic areas and of the orbital areas (with the exception of the lateral part of the orbital area, in which ^{18}F-FDG uptake decreased only in the right side). Also, ^{18}F-FDG uptake decreased in the right frontal pole, the primary visual area and agranular insular area, and in the left anterior cingulate area. In primary somatosensory areas, the ^{18}F-FDG uptake showed mixed responses; for instance, it increased in the left side of the mouth area whereas it decreased in the right side of the upper limb area. The ^{18}F-FDG uptake decreased, with different laterality, in most the olfactory areas, with the exception of the main olfactory bulb, in which ^{18}F-FDG uptake increased in the left side and decreased in the right side. The ^{18}F-FDG uptake decreased in left and right CA1 and CA3 of the hippocampus, in the right dentate gyrus and in the left retrohippocampal region, endopiriform nucleus, and basolateral amygdalar nucleus. In the striatum, ^{18}F-FDG uptake decreased in the right ventral striatum, which includes the nucleus accumbens and the olfactory tubercle, in the left striatum-like amygdalar nuclei and in both sides of the caudoputamen. In the pallidum, ^{18}F-FDG uptake decreased in the left internal segment of the globus pallidus, in the right magnocellular nucleus and in both sides of the substantia innominata. Also, ^{18}F-FDG uptake

decreased in the right sensory-motor related cortex of the thalamus, in the right external nucleus of the inferior colliculus of the midbrain, and in both sides of the lateral hypothalamic area. ^{18}F-FDG uptake decreased in two regions of the pons: the right behavioral state related area, and both sides of the pontine central gray. In the medulla, ^{18}F-FDG uptake showed mixed responses: increased in the right sensory-related areas and decreased in both sides of some motor-related areas (e.g., the paragigantocellular reticular nucleus, the perihypoglossal nuclei and the vestibular nuclei). In the cerebellum, ^{18}F-FDG uptake decreased in both sides of two vermal regions (e.g., culmen and declive, VI) and increased in the right central lobule of the vermal regions as well as in some right hemispheric regions (e.i., simple lobule, copula pyramidis and paraflocculus) and cerebellar nuclei.

In the ~20-30 min post-treatment time window, ghrelin treatment mainly increased ^{18}F-FDG uptake in specific brain areas. In the isocortex, ^{18}F-FDG uptake increased in the left side of several somatosensory areas (plus the right side of the mouth area), of the auditory areas and of the temporal association areas as well as in the right side of the anteromedial visual area, of some retrosplenial areas, and of posterior parietal association areas. In the isocortex, ^{18}F-FDG uptake also increased in both sides of the infralimbic area and of the medial part of the orbital area, whereas increased only in the left side of the lateral and ventrolateral parts of the orbital area. The ^{18}F-FDG uptake also increased in both sides of two olfactory areas (i.e., the dorsal part of the taenia tecta, and the dorsal peduncular area) and in the right side of several areas of the hippocampal formation (including also the left side of the CA1). In the striatum, ^{18}F-FDG uptake increased in both sides of the caudoputamen and the lateral septal nucleus, in the left nucleus accumbens, and in the right striatum-like amygdalar nuclei. The uptake of ^{18}F-FDG increased both sides of some regions of the dorsal, ventral, medial and caudal pallidum. In the thalamus, ^{18}F-FDG uptake increased in the right the sensory-motor cortex related area as well as in most of the right polymodal association cortex related areas. In the hypothalamus, ^{18}F-FDG uptake increased in both sides of the periventricular zone and in the right lateral zone. In the midbrain, ^{18}F-FDG uptake increased in the right ventral tegmental area, reticular nucleus, reticular part of the substantia nigra and behavioral-related areas, in the left motor-related area of the superior colliculus, as well as in both sides of the periaqueductal gray and of the pretectal regions. In the medulla, ^{18}F-FDG uptake decreased in the right sensory-related areas. In the cerebellum, ^{18}F-FDG uptake increased several left vermal regions [Central lobule, Culmen, Declive (VI), Pyramus (VIII), Uvula (IX), Nodulus (X)], in the left copula pyramidis and in the

left cerebellar nuclei. At the same time, ^{18}F-FDG uptake decreased in two hemispheric regions: the right flocculus and both sides of the paraflocculus.

Systemically-injected Fr-ghrelin gains access to brain areas known to contain fenestrated capillaries. To investigate whether circulating ghrelin could differentially access the right and left sides of the brain, mice were systemically-injected with Fr-ghrelin and euthanized at 15 min after treatment. Brains were then processed, and the localization of Fr-ghrelin was imaged in the coronal brain sections using a filter set for far-red emission. Fr-ghrelin signal was observed in the epithelial cells of the choroid plexus (CP), as previously reported [30], as well as in cells of several midline structures containing fenestrated capillaries, including the subfornical organ (SFO), the subcommissural organ (SCO), the organum vasculosum of the lamina terminalis (OVLT) and the AP (Fig. 6 A-E). Fr-ghrelin signal was not detected in other brain areas protected by the blood-brain-barrier, such as the olfactory bulbs (not shown), the ventral tegmental area (not shown) or the hippocampus (Fig. 6 F). As compared to the signal found in the brain sections of vehicle-treated mice, fluorescent signal was also detected in the ARH of Fr-ghrelin-treated mice (Fig. 6 G-H). Notably, Fr-ghrelin signal in the right and the left ARH of Fr-ghrelin-treated mice were not statistically different (Fig. 6 I).

Systemically injected ghrelin induces a similar induction of c-Fos in the left and right ARH. To investigate whether circulating ghrelin could differentially activate the right and left ARH, mice were systemically-injected with ghrelin and euthanized at 2 h after treatment. Brains were then processed, and immuno-stained for c-Fos. As previously reported [23], we confirmed that the number of c-Fos-IR cells significantly increased only in the ARH of ghrelin-treated mice, as compared to the number of c-Fos-IR cells detected in the ARH of vehicle-treated mice (Fig. 7 A-B). Still, the number of c-Fos-IR cells in the right and the left ARH of ghrelin-treated mice were not statistically different (Fig. 7 C).

DISCUSSION

We show here that ghrelin treatment induces rapid, transient and asymmetric changes in the metabolic activity of the brain of male mice. In contrast, treatment with fluorescent ghrelin results in a non-asymmetric labeling of most brain areas with fenestrated capillaries, and ghrelin treatment induces a symmetric elevation of c-Fos expression at the ARH. Thus, systemically-injected ghrelin recruits most central neuronal networks in an asymmetric fashion in male mice, and the neurobiological basis of such asymmetry seems to be independent of the accessibility of ghrelin into the brain or the rapid action of ghrelin at the ARH level.

To our knowledge, the current study provides the first assessment of food intake-independent ghrelin-induced changes of the ^{18}F-FDG uptake in the mouse brain. Preclinical-PET is a powerful non-invasive and quantitative technology that generates a three-dimensional nuclear imaging data set and allows the assessment of functional processes in specific brain areas of live animals [48]. Importantly, preclinical-PET displays low spatial and temporal resolutions that must be considered when interpreting results. Indeed, such low resolution of preclinical-PET studies together with the fact that we found that ghrelin affected glucose metabolism in many brain areas that are highly interconnected undermined our capability to delineate a precise and sequential neuronal circuit recruited by ghrelin. Given the limits in spatial resolution, current studies may have also failed to reveal changes in the ^{18}F-FDG uptake when different cells displayed simultaneous increase and decrease of glucose metabolism within the same brain area. Finally, results presented here should be interpreted as average responses due to the group-wise statistical analysis performed. Despite all these considerations, the current study resulted in a valuable strategy that provided an alternative analysis of the central targets of circulating ghrelin.

In line with the notion that ghrelin treatment induces neuroendocrine effects, we found that ghrelin also affects glucose metabolism in the hypothalamus. Specifically, ghrelin induced a symmetric reduction of the glucose metabolism in both sides of the hypothalamic lateral zone in the 10-to-20 min posttreatment period whereas increased the glucose metabolism in periventricular zone of the hypothalamus, which includes the paraventricular nucleus and the ARH, in the 20-to-30 min posttreatment period. Also, ghrelin treatment affected the glucose metabolism in several brain areas that are known to control the autonomic function, including specific areas, such as the agranular insular area, the anterior

cingulate area and the basolateral amygdala, or larger brain regions, such as the hypothalamus, nuclei of the pons or the medulla, in which the specific area responsive to ghrelin could not be precisely identified due to the low spatial resolution of the preclinical-PET [49,50]. Ghrelin increased the glucose metabolism in both sides of the periaqueductal gray that regulates not only autonomic function, but also motivated behaviors.

Ghrelin affects complex functions such as the ability to process information of the pleasurable (hedonic) value of rewarding stimuli or the actions to seek them [17,51]. Here, we found that ghrelin affected brain metabolism in structures of the limbic system, such as the nucleus accumbens, in the right ventral tegmental area and in the ventral pallidum (both sides of substantia innominate and the right magnocellular nucleus). The nucleus accumbens is involved in cognitive processing of motivation, reward and reinforcement learning. The nucleus accumbens receives innervations from the prefrontal cortex (the prelimbic and infralimbic cortex), the ventral hippocampus, the midline thalamic nuclei, the intralaminar nuclei of the thalamus and the ventral tegmental area, and strongly innervates the ventral pallidum. The ventral pallidum controls the processing and execution of motivated behaviors [52]: it receives inputs from the nucleus accumbens, as well as from the ventral tegmental area, and projects to the medial dorsal nucleus of the dorsal thalamus, which in turn projects to the prefrontal cortex and the ventral striatum [53,54]. Ghrelin treatment also increased glucose metabolism in other brain areas related to the mesolimbic system such as the dorsal thalamus as well as the prelimbic, limbic, frontal pole, orbital and cortical amygdalar areas of the cerebral cortex. Also, ghrelin rapidly reduced glucose metabolism in the olfactory tubercle, which is located in the ventral striatum and is a processing center that translates sensory and rewarding information into subsequent goal-directed behaviors [55]. The olfactory tubercle receives primary innervations from the olfactory bulbs and the ventral tegmental area and it is highly interconnected with the nucleus accumbens, the ventral pallidum and other centers of the basal ganglia. The olfactory tubercle also recruits the striatum-like amygdalar nuclei [55], that showed decreased glucose metabolism in response to ghrelin. Of note, ghrelin decreases glucose metabolism in the hypothalamic lateral zone, which receives numerous innervations and projects to different center of the limbic system, including the ventral pallidum, the ventral tegmental area and the nucleus accumbens [56]. In line with the reports indicating that ghrelin affects memory and learning, we found that ghrelin also affected the glucose metabolism in the Ammon's horns and in the dentate gyrus of the hippocampus. The hippocampus plays a major role in the formation of spatial representations and episodic

memory, and its crosstalk with the mesolimbic pathway helps to control reward associative processes important for memory-guided decision-making [57]. The hippocampus receives innervations from the ventral tegmental area, and indirectly innervates the ventral tegmental area via the nucleus accumbens and the ventral pallidum.

We found that ghrelin treatment rapidly affected the glucose metabolism in brain areas that are part of the basal ganglia, which are a collection of interconnected subcortical brain nuclei integrated to cortico-basal ganglia-thalamo-cortical loops that modulate not only voluntary motor actions but also learning, working memory, decision making and reward processing [58,59]. These functional loops include motor, associative and limbic loops that converge, integrate and exchange information, at different levels, in order to control complex goal-directed behaviors [59]. The larger center of the basal ganglia is the striatum, which is considered an input area [60]. Here, ghrelin increased glucose metabolism not only in the ventral (nucleus accumbens and olfactory tubercle) striatum, as discussed above, but also in the dorsal (caudoputamen) striatum. The dorsal striatum receives innervations from the cerebral cortex (corticostriatal projections), the thalamus (thalamostriatal projections), the SNC (nigrostriatal projections) and the ventral tegmental area (mesostriatal projections), among others [60]. Interestingly, ghrelin rapidly increases glucose metabolism in cortical motor areas, which originate corticostriatal projections, and in the intralaminar nuclei of the dorsal thalamus, which originate most thalamostriatal projections [61]. The striatum projects to other basal ganglia: the reticular part of the substantia nigra and the external and internal globus pallidus of the dorsal pallidum. The external globus pallidus projects to the subthalamic nucleus that, in turn, project to the internal globus pallidus and the reticular part of the substantia nigra, which are the major output nuclei of the motor loop via their projections to thalamic nuclei [60]. We found that ghrelin decreases glucose metabolism in the internal globus pallidus whereas increases the glucose metabolism in the reticular part of the substantia nigra, in the external globus pallidus, and in some nuclei of the dorsal thalamus. These thalamic nuclei act as relay stations between the basal ganglia and the cerebral cortex in order to close motor and associative loops. In the 10-to-20 min period, ghrelin decreased glucose metabolism in primary and secondary motor areas, suggesting that these areas are controlled in a dynamic fashion.

Ghrelin treatment also affected glucose metabolism in brainstem areas that belong to the reticular formation, which is an interconnected network of brain nuclei that serve as a major integration and relay system to coordinate functions essential for life. The reticular

formation projects to both the cerebral cortex, via the ascending reticular activating system in order to sort sensory stimuli and to maintain behavioral arousal and consciousness, as well as to the spinal cord, via the reticulospinal tracts in order to play premotor functions on the control of movements and to control of respiratory and cardiovascular functions. Among the areas that are part of the reticular formation, ghrelin changed the glucose metabolism in the midbrain reticular nucleus, the perihypoglossal nuclei, the gigantocellular reticular nucleus as well as in another less defined behavioral state-, motor- and sensory-related areas of the brain stem. Also, ghrelin affects the glucose metabolism in some layers the inferior and superior colliculus, which project to the paramedian pontine reticular formation, and in vermal and hemispheric regions of the cerebellum, which are reciprocally connected to the reticular formation via the inferior cerebellar peduncles and help integrate visual, auditory, and vestibular stimuli in motor coordination.

Since preclinical-PET studies showed that ghrelin induces asymmetric changes on the metabolic mouse brain activity, we evaluated the accessibility of systemically injected Fr-ghrelin into the entire mouse brain, and found that Fr-ghrelin labels the CP, the ARH, the AP, the SFO and the OVLT, all of which contain fenestrated capillaries and express GHSR [31,62,63]. Among the brain labeled areas labeled in our experimental conditions, the ARH is only a bilateral structure, located each side of the third ventricle, and we found that Fr-ghrelin labeled with similar intensity both of its sides. Of note, systemically-injected radiolabeled ghrelin was also shown to label the olfactory bulb in the mouse brain [21,64], in line with the notion that the OB contains a permeable blood-brain-barrier [65,66]. Despite the OB, as well as other odor-processing brain regions, seem to contains GHSR-expressing cells [7,67,68], we failed to detect Fr-ghrelin labeling in the OB nor in any other brain area lacking fenestrated capillaries. Thus, circulating Fr-ghrelin seems to quickly gain access to a limited number of brain regions, as we and others have observed before using different fluorescent ghrelin analogs and additional strategies that include enzymatic amplification steps aimed to enhance the signal of the tracers [23,25,26]. Of note, the size of the brain areas that were labeled with systemically-injected Fr-ghrelin is below the spatial resolution of the preclinical-PET strategy, and, consequently, the extent to which ghrelin affects its ^{18}F-FDG uptake could not be determined with the current methodology. As an alternative strategy to test the putative asymmetry in the central effects of ghrelin, we assessed if systemically-injected ghrelin induces an asymmetric increase of the marker of neuronal activation c-Fos in the ARH, the key hypothalamic region mediating the orexigenic effect of

ghrelin [42], and found no evidence of laterality. Thus, systemically-injected ghrelin does not seem to display an asymmetric accessibility or induction of c-Fos in the ARH.

Notably, ghrelin treatment in humans also induces asymmetric effects on blood-oxygen-level dependent signal in brain areas associated to motor and limbic systems [69–74]. Thus, the mechanisms underlying the region-specific functional lateralization of the human brain in response to ghrelin may be clarified using mice as an experimental model. For instance, it is well established that systemically-injected ghrelin in mice mainly targets the ARH, which could, consequently, recruit other areas with some degree of lateralization. Within the ARH, ghrelin mainly acts on neurons producing agouti-related protein (AgRP), which are required and sufficient to mediate the orexigenic effects of ghrelin [24,26,75]. AgRP neurons innervate many brain areas in which we detected changes of the glucose metabolism, including the reticular part of the substantia nigra, the olfactory areas, the medial amygdalar nucleus, the ventral pallidum, the lateral hypothalamic area and the ventral tegmental area [76–80]. Thus, AgRP neurons of the ARH could be responsible of some of the observed effects of ghrelin on brain glucose metabolism; however, it remains to be determined if the projections from the ARH display some degree of lateralization. Importantly, the asymmetric effects of ghrelin on the metabolic brain activity may result from the inherent lateralization of some brain functions [81]. For instance, mesolimbic system in rats show inherent functional lateralization as indicated by the observations that the right cortex and nucleus accumbens contain higher basal levels of DA, as compared to the left structures, and that the right nucleus accumbens receives greater dopaminergic neurotransmission, as compared to the left nucleus accumbens, in response to cerebellar stimulation [82,83]. Also, some limbic centers in rats display unilateral ^{18}F-FDG uptake in response to the systemic administration of an opioid receptor agonist [84]. Similarly, the anterior cingulate shows asymmetric metabolism of the endogenous opioid peptides in humans [85]. In humans and rodents, the hypothalamic control of some neuroendocrine systems and food intake was also shown to display some degree a functional asymmetry [86,87]. Alternatively, the asymmetric effects of ghrelin on the brain glucose metabolism might be due to the action of the hormone on the peripheral fibers of the autonomic nervous system (e.g. vagus nerve [88]), which show anatomical asymmetry due to the differential innervation of the organs located in the left and right sides of the thoracic and abdominal cavities [89]. Further studies in mice would likely help to better understand the neurobiological basis of the asymmetric effects of ghrelin on the brain metabolism.

In conclusion, our study provides an alternative systematic analysis of the brain areas responsive to ghrelin treatment in male mice. The study unmasks several central targets of ghrelin in the mouse brain that had not been described before, and provides the first indication that the central actions of ghrelin display asymmetric effects, in a food intake-independent manner. We hope the current detailed map of the ghrelin-responsive brain areas will be a valuable tool for the future delineation of the neuronal circuits that mediate the different neuroendocrine, autonomic and behavioral actions of ghrelin. Future studies will be required to investigate the extent to which current observations regarding the actions of ghrelin in male mice apply to female mice.

STATEMENTS

Acknowledgement: We would like to thank to Mirta Reynaldo, Guadalupe García Romero, Josefina Lacunza and Lucas Aguilar, for their technical assistance.

Statement of Ethics: This study protocol was reviewed and approved by the Institutional Animal Care and Use Committee of the Multidisciplinary Institute of Cell Biology, approval ID 17-0221.

Conflict of Interest Statement: The authors have no conflicts of interest to declare.

Funding Sources: This work was supported by grants to MP from: Fondo para la Investigación Científica y Tecnológica (FONCyT, PICT2017-3196, PICT2019-3054 and PICT2020-3270), CONICET (PUE105) and National Qatar Research Foundation (NPRP13S-0209-200315). Sponsors did not participate in the generation of data or preparation of the manuscript.

Author Contributions: Gimena Fernandez, Maia Uriarte, Leandro Urrutia, Magdalena Ponce de León and Gimena Fernandez carried out the experiment. Pablo Nicolás De Francesco, Gimena Fernandez, Maia Uriarte, Leandro Urrutia, Magdalena Ponce de León and German Falasco analyzed the data. Jean-Alain Fehrentz generated key reagents and provided critical feedback. Pablo Nicolás De Francesco and Mario Perello conceived the original idea and wrote the manuscript. All authors discussed the results and contributed to the final manuscript.

Data Availability Statement: All data generated or analyzed during this study are included in this article. Further enquiries can be directed to the corresponding author.

REFERENCES

1 Kojima M, Kangawa K. Ghrelin: from gene to physiological function. Results Probl Cell Differ. 2010;50:185–205.

2 Cummings DE. Ghrelin and the short- and long-term regulation of appetite and body weight. Physiol Behav. 2006 Aug;89(1):71–84.

3 Zhao T-J, Liang G, Li RL, Xie X, Sleeman MW, Murphy AJ, et al. Ghrelin O-acyltransferase (GOAT) is essential for growth hormone-mediated survival of calorie-restricted mice. Proc Natl Acad Sci USA. 2010 Apr;107(16):7467–72.

4 Gorwood P, Blanchet-Collet C, Chartrel N, Duclos J, Dechelotte P, Hanachi M, et al. New Insights in Anorexia Nervosa. Front Neurosci. 2016;10:256.

5 Maria Monteleone A, Monteleone P, Dalle Grave R, Nigro M, El Ghoch M, Calugi S, et al. Ghrelin response to hedonic eating in underweight and short-term weight restored patients with anorexia nervosa. Psychiatry Res. 2016 Jan;235:55–60.

6 Mihalache L, Gherasim A, Niţă O, Ungureanu MC, Pădureanu SS, Gavril RS, et al. Effects of ghrelin in energy balance and body weight homeostasis. Hormones (Athens). 2016 Feb;15(2):186–96.

7 Mani BK, Walker AK, Lopez Soto EJ, Raingo J, Lee CE, Perelló M, et al. Neuroanatomical characterization of a growth hormone secretagogue receptor-green fluorescent protein reporter mouse. J Comp Neurol. 2014 Nov;522(16):3644–66.

8 Cruz CRY, Smith RG. The growth hormone secretagogue receptor. Vitam Horm. 2008;77:47–88.

9 Ariyasu H, Takaya K, Tagami T, Ogawa Y, Hosoda K, Akamizu T, et al. Stomach is a major source of circulating ghrelin, and feeding state determines plasma ghrelin-like immunoreactivity levels in humans. J Clin Endocrinol Metab. 2001 Oct;86(10):4753–8.

10 Hataya Y, Akamizu T, Takaya K, Kanamoto N, Ariyasu H, Saijo M, et al. A low dose of ghrelin stimulates growth hormone (GH) release synergistically with GH-releasing hormone in humans. J Clin Endocrinol Metab. 2001 Sep;86(9):4552.

11 Cabral A, Suescun O, Zigman JM, Perello M. Ghrelin indirectly activates hypophysiotropic CRF neurons in rodents. PLoS ONE. 2012;7(2):e31462.

12 Cabral A, Portiansky E, Sánchez-Jaramillo E, Zigman JM, Perello M. Ghrelin activates hypophysiotropic corticotropin-releasing factor neurons independently of the arcuate nucleus. Psychoneuroendocrinology. 2016 May;67:27–39.

13 Zizzari P, Hassouna R, Grouselle D, Epelbaum J, Tolle V. Physiological roles of preproghrelin-derived peptides in GH secretion and feeding. Peptides. 2011 Nov;32(11):2274–82.

14 Popovic V, Miljic D, Micic D, Damjanovic S, Arvat E, Ghigo E, et al. Ghrelin main action on the regulation of growth hormone release is exerted at hypothalamic level. J Clin Endocrinol Metab. 2003 Jul;88(7):3450–3.

15 Steyn FJ, Tolle V, Chen C, Epelbaum J. Neuroendocrine Regulation of Growth Hormone Secretion. Compr Physiol. 2016 Mar;6(2):687–735.

16 Mani BK, Shankar K, Zigman JM. Ghrelin's Relationship to Blood Glucose. Endocrinology. 2019 May;160(5):1247–61.

17 Perello M, Dickson SL. Ghrelin signalling on food reward: a salient link between the gut and the mesolimbic system. J Neuroendocrinol. 2015 Jun;27(6):424–34.

18 Nagaya N, Miyatake K, Uematsu M, Oya H, Shimizu W, Hosoda H, et al. Hemodynamic, renal, and hormonal effects of ghrelin infusion in patients with chronic heart failure. J Clin Endocrinol Metab. 2001 Dec;86(12):5854–9.

19 Levin F, Edholm T, Ehrström M, Wallin B, Schmidt PT, Kirchgessner AM, et al. Effect of peripherally administered ghrelin on gastric emptying and acid secretion in the rat. Regul Pept. 2005 Nov;131(1–3):59–65.

20 Kishimoto I, Tokudome T, Hosoda H, Miyazato M, Kangawa K. Ghrelin and cardiovascular diseases. J Cardiol. 2012 Jan;59(1):8–13.

21 Diano S, Farr SA, Benoit SC, McNay EC, da Silva I, Horvath B, et al. Ghrelin controls hippocampal spine synapse density and memory performance. Nat Neurosci. 2006 Mar;9(3):381–8.

22 Harmatz ES, Stone L, Lim SH, Lee G, McGrath A, Gisabella B, et al. Central Ghrelin Resistance Permits the Overconsolidation of Fear Memory. Biol Psychiatry. 2017 15;81(12):1003–13.

23 Cabral A, Valdivia S, Fernandez G, Reynaldo M, Perello M. Divergent neuronal circuitries underlying acute orexigenic effects of peripheral or central ghrelin: critical role of brain accessibility. J Neuroendocrinol. 2014 Aug;26(8):542–54.

24 Cabral A, De Francesco PN, Perello M. Brain circuits mediating the orexigenic action of peripheral ghrelin: narrow gates for a vast kingdom. Front Endocrinol (Lausanne). 2015;6:44.

25 Perello M, Cabral A, Cornejo MP, De Francesco PN, Fernandez G, Uriarte M. Brain accessibility delineates the central effects of circulating ghrelin. J Neuroendocrinol. 2019 Jul;31(7):e12677.

26 Schaeffer M, Langlet F, Lafont C, Molino F, Hodson DJ, Roux T, et al. Rapid sensing of circulating ghrelin by hypothalamic appetite-modifying neurons. Proceedings of the National Academy of Sciences. 2013 Jan;110:1512–7.

27 Ciofi P. The arcuate nucleus as a circumventricular organ in the mouse. Neurosci Lett. 2011 Jan;487(2):187–90.

28 Cabral A, Cornejo MP, Fernandez G, De Francesco PN, Garcia-Romero G, Uriarte M, et al. Circulating Ghrelin Acts on GABA Neurons of the Area Postrema and Mediates Gastric Emptying in Male Mice. Endocrinology. 2017 May;158(5):1436–49.

29 Banks WA. Extent and Direction of Ghrelin Transport Across the Blood-Brain Barrier Is Determined by Its Unique Primary Structure. Journal of Pharmacology and Experimental Therapeutics. 2002 Aug;302(2):822–7.

30 Uriarte M, De Francesco PN, Fernandez G, Cabral A, Castrogiovanni D, Lalonde T, et al. Evidence Supporting a Role for the Blood-Cerebrospinal Fluid Barrier Transporting Circulating Ghrelin into the Brain. Mol Neurobiol. 2018 Oct DOI: 10.1007/s12035-018-1362-8

31 Uriarte M, De Francesco PN, Fernández G, Castrogiovanni D, D'Arcangelo M, Imbernon M, et al. Circulating ghrelin crosses the blood-cerebrospinal fluid barrier via growth hormone secretagogue receptor dependent and independent mechanisms. Mol Cell Endocrinol. 2021 Dec;538:111449.

32 Cabral A, Fernandez G, Perello M. Analysis of brain nuclei accessible to ghrelin present in the cerebrospinal fluid. Neuroscience. 2013 Dec;253:406–15.

33 Hewson AK, Dickson SL. Systemic administration of ghrelin induces Fos and Egr-1 proteins in the hypothalamic arcuate nucleus of fasted and fed rats. J Neuroendocrinol. 2000 Nov;12(11):1047–9.

34 Wang L, Saint-Pierre DH, Taché Y. Peripheral ghrelin selectively increases Fos expression in neuropeptide Y - synthesizing neurons in mouse hypothalamic arcuate nucleus. Neurosci Lett. 2002 May;325(1):47–51.

35 Rüter J, Kobelt P, Tebbe JJ, Avsar Y, Veh R, Wang L, et al. Intraperitoneal injection of ghrelin induces Fos expression in the paraventricular nucleus of the hypothalamus in rats. Brain Res. 2003 Nov;991(1–2):26–33.

36 Takayama K, Johno Y, Hayashi K, Yakabi K, Tanaka T, Ro S. Expression of c-Fos protein in the brain after intravenous injection of ghrelin in rats. Neurosci Lett. 2007 May;417(3):292–6.

37 Kobelt P, Wisser A-S, Stengel A, Goebel M, Inhoff T, Noetzel S, et al. Peripheral injection of ghrelin induces Fos expression in the dorsomedial hypothalamic nucleus in rats. Brain Res. 2008 Apr;1204:77–86.

38 Cornejo MP, Barrile F, De Francesco PN, Portiansky EL, Reynaldo M, Perello M. Ghrelin Recruits Specific Subsets of Dopamine and GABA Neurons of Different Ventral Tegmental Area Sub-nuclei. Neuroscience. 2018 Sep DOI: 10.1016/j.neuroscience.2018.09.027

39 Hoffman GE, Lyo D. Anatomical markers of activity in neuroendocrine systems: are we all "fos-ed out"? J Neuroendocrinol. 2002 Apr;14(4):259–68.

40 de Souza GO, Wasinski F, Donato J. Characterization of the metabolic differences between male and female C57BL/6 mice. Life Sci. 2022 May;301:120636.

41 Barrile F, M'Kadmi C, De Francesco PN, Cabral A, García Romero G, Mustafá ER, et al. Development of a novel fluorescent ligand of growth hormone secretagogue receptor based on the N-Terminal Leap2 region. Mol Cell Endocrinol. 2019 01;498:110573.

42 Cornejo MP, Denis RGP, García Romero G, Fernández G, Reynaldo M, Luquet S, et al. Ghrelin treatment induces rapid and delayed increments of food intake: a heuristic model to explain ghrelin's orexigenic effects. Cell Mol Life Sci. 2021 Oct;78(19–20):6689–708.

43 Reference Space — Allen SDK dev documentation [Internet]. [cited 2022 Jan 16]. Available from: https://allensdk.readthedocs.io/en/latest/reference_space.html

44 Schindelin J, Arganda-Carreras I, Frise E, Kaynig V, Longair M, Pietzsch T, et al. Fiji: an open-source platform for biological-image analysis. Nat Methods. 2012 Jul;9(7):676–82.

45 Cardona A, Saalfeld S, Schindelin J, Arganda-Carreras I, Preibisch S, Longair M, et al. TrakEM2 software for neural circuit reconstruction. PLoS ONE. 2012;7(6):e38011.

46 Paxinos G, Franklin KBJ. The mouse brain in stereotaxic coordinates. 2nd ed. San Diego: Academic Press; 2001.

47 Wang Q, Ding S-L, Li Y, Royall J, Feng D, Lesnar P, et al. The Allen Mouse Brain Common Coordinate Framework: A 3D Reference Atlas. Cell. 2020 May;181(4):936-953.e20.

48 Boehm MA, Bonaventura J, Gomez JL, Solís O, Stein EA, Bradberry CW, et al. Translational PET applications for brain circuit mapping with transgenic neuromodulation tools. Pharmacol Biochem Behav. 2021 May;204:173147.

49 McDonald AJ. Functional neuroanatomy of the basolateral amygdala: Neurons, neurotransmitters, and circuits. Handb Behav Neurosci. 2020;26:1–38.

50 Nagai M, Hoshide S, Kario K. The insular cortex and cardiovascular system: a new insight into the brain-heart axis. J Am Soc Hypertens. 2010 Aug;4(4):174–82.

51 Cornejo MP, Mustafá ER, Barrile F, Cassano D, De Francesco PN, Raingo J, et al. THE INTRIGUING LIGAND-DEPENDENT AND LIGAND-INDEPENDENT ACTIONS OF THE GROWTH HORMONE SECRETAGOGUE RECEPTOR ON REWARD-RELATED BEHAVIORS. Neurosci Biobehav Rev. 2021 Jan;120:401–16.

52 Root DH, Melendez RI, Zaborszky L, Napier TC. The ventral pallidum: Subregion-specific functional anatomy and roles in motivated behaviors. Prog Neurobiol. 2015 Jul;130:29–70.

53 Pierce RC, Kumaresan V. The mesolimbic dopamine system: the final common pathway for the reinforcing effect of drugs of abuse? Neurosci Biobehav Rev. 2006;30(2):215–38.

54 Ikemoto S. Brain reward circuitry beyond the mesolimbic dopamine system: a neurobiological theory. Neurosci Biobehav Rev. 2010 Nov;35(2):129–50.

55 Xiong A, Wesson DW. Illustrated Review of the Ventral Striatum's Olfactory Tubercle. Chem Senses. 2016;41(7):549–55.

56 Castro DC, Berridge KC. Advances in the neurobiological bases for food "liking" versus "wanting." Physiol Behav. 2014 Sep;136:22–30.

57 Hyman SE, Malenka RC, Nestler EJ. Neural mechanisms of addiction: the role of reward-related learning and memory. Annu Rev Neurosci. 2006;29:565–98.

58 Arsalidou M, Duerden EG, Taylor MJ. The centre of the brain: topographical model of motor, cognitive, affective, and somatosensory functions of the basal ganglia. Hum Brain Mapp. 2013 Nov;34(11):3031–54.

59 Simonyan K. Recent advances in understanding the role of the basal ganglia. F1000Res. 2019;8. DOI: 10.12688/f1000research.16524.1

60 Lanciego JL, Luquin N, Obeso JA. Functional neuroanatomy of the basal ganglia. Cold Spring Harb Perspect Med. 2012 Dec;2(12):a009621.

61 Groenewegen HJ, Berendse HW. The specificity of the “nonspecific” midline and intralaminar thalamic nuclei. Trends Neurosci. 1994 Feb;17(2):52–7.

62 Hoyda TD, Smith PM, Ferguson AV. Gastrointestinal hormone actions in the central regulation of energy metabolism: potential sensory roles for the circumventricular organs. Int J Obes (Lond). 2009 Apr;33 Suppl 1:S16-21.

63 Fry M, Ferguson AV. Ghrelin: central nervous system sites of action in regulation of energy balance. Int J Pept. 2010;2010:616757.

64 Rhea EM, Salameh TS, Gray S, Niu J, Banks WA, Tong J. Ghrelin transport across the blood-brain barrier can occur independently of the growth hormone secretagogue receptor. Mol Metab. 2018;18:88–96.

65 Ueno M, Akiguchi I, Naiki H, Fujibayashi Y, Fukuyama H, Kimura J, et al. The persistence of high uptake of serum albumin in the olfactory bulbs of mice throughout their adult lives. Arch Gerontol Geriatr. 1991 Oct;13(2):201–9.

66 Ueno M, Dobrogowska DH, Vorbrodt AW. Immunocytochemical evaluation of the blood-brain barrier to endogenous albumin in the olfactory bulb and pons of senescence-accelerated mice (SAM). Histochem Cell Biol. 1996 Mar;105(3):203–12.

67 Jiang H, Betancourt L, Smith RG. Ghrelin amplifies dopamine signaling by cross talk involving formation of growth hormone secretagogue receptor/dopamine receptor subtype 1 heterodimers. Mol Endocrinol. 2006 Aug;20(8):1772–85.

68 Tong J, Mannea E, Aimé P, Pfluger PT, Yi C-X, Castaneda TR, et al. Ghrelin enhances olfactory sensitivity and exploratory sniffing in rodents and humans. J Neurosci. 2011 Apr;31(15):5841–6.

69 Han JE, Frasnelli J, Zeighami Y, Larcher K, Boyle J, McConnell T, et al. Ghrelin Enhances Food Odor Conditioning in Healthy Humans: An fMRI Study. Cell Rep. 2018 04;25(10):2643-2652.e4.

70 Malik S, McGlone F, Bedrossian D, Dagher A. Ghrelin modulates brain activity in areas that control appetitive behavior. Cell Metab. 2008 May;7(5):400–9.

71 Jones RB, McKie S, Astbury N, Little TJ, Tivey S, Lassman DJ, et al. Functional neuroimaging demonstrates that ghrelin inhibits the central nervous system response to ingested lipid. Gut. 2012 Nov;61(11):1543–51.

72 Goldstone AP, Prechtl CG, Scholtz S, Miras AD, Chhina N, Durighel G, et al. Ghrelin mimics fasting to enhance human hedonic, orbitofrontal cortex, and hippocampal responses to food. Am J Clin Nutr. 2014 Jun;99(6):1319–30.

73 Kunath N, Müller NCJ, Tonon M, Konrad BN, Pawlowski M, Kopczak A, et al. Ghrelin modulates encoding-related brain function without enhancing memory formation in humans. Neuroimage. 2016 Nov;142:465–73.

74 Farokhnia M, Grodin EN, Lee MR, Oot EN, Blackburn AN, Stangl BL, et al. Exogenous ghrelin administration increases alcohol self-administration and modulates brain functional activity in heavy-drinking alcohol-dependent individuals. Mol Psychiatry. 2018;23(10):2029–38.

75 Chen VP, Gao Y, Geng L, Brimijoin S. Radiometric assay of ghrelin hydrolase activity and 3H-ghrelin distribution into mouse tissues. Biochem Pharmacol. 2015 Dec;98(4):732–9.

76 Broberger C, Johansen J, Johansson C, Schalling M, Hökfelt T. The neuropeptide Y/agouti gene-related protein (AGRP) brain circuitry in normal, anorectic, and monosodium glutamate-treated mice. Proc Natl Acad Sci USA. 1998 Dec;95(25):15043–8.

77 Wu Q, Boyle MP, Palmiter RD. Loss of GABAergic signaling by AgRP neurons to the parabrachial nucleus leads to starvation. Cell. 2009 Jun;137(7):1225–34.

78 Dietrich MO, Horvath TL. Fat incites tanycytes to neurogenesis. Nat Neurosci. 2012 May;15(5):651–3.

79 Betley JN, Cao ZFH, Ritola KD, Sternson SM. Parallel, redundant circuit organization for homeostatic control of feeding behavior. Cell. 2013 Dec;155(6):1337–50.

80 Wang D, He X, Zhao Z, Feng Q, Lin R, Sun Y, et al. Whole-brain mapping of the direct inputs and axonal projections of POMC and AgRP neurons. Front Neuroanat. 2015;9:40.

81 Sullivan RM. Hemispheric asymmetry in stress processing in rat prefrontal cortex and the role of mesocortical dopamine. Stress. 2004 Jun;7(2):131–43.

82 Rosen GD, Finklestein S, Stoll AL, Yutzey DA, Denenberg VH. Neurochemical asymmetries in the albino rat's cortex, striatum, and nucleus accumbens. Life Sci. 1984 Mar;34(12):1143–8.

83 Holloway ZR, Paige NB, Comstock JF, Nolen HG, Sable HJ, Lester DB. Cerebellar Modulation of Mesolimbic Dopamine Transmission Is Functionally Asymmetrical. Cerebellum. 2019 Oct;18(5):922–31.

84 Hooker JM, Patel V, Kothari S, Schiffer WK. Metabolic changes in the rodent brain after acute administration of salvinorin A. Mol Imaging Biol. 2009 Jun;11(3):137–43.

85 Watanabe H, Fitting S, Hussain MZ, Kononenko O, Iatsyshyna A, Yoshitake T, et al. Asymmetry of the endogenous opioid system in the human anterior cingulate: a putative molecular basis for lateralization of emotions and pain. Cereb Cortex. 2015 Jan;25(1):97–108.

86 Gerendai I, Halász B. Asymmetry of the neuroendocrine system. News Physiol Sci. 2001 Apr;16:92–5.

87 Kiss DS, Toth I, Jocsak G, Bartha T, Frenyo LV, Barany Z, et al. Metabolic Lateralization in the Hypothalamus of Male Rats Related to Reproductive and Satiety States. Reprod Sci. 2020 May;27(5):1197–205.

88 Perelló M, Cornejo MP, De Francesco PN, Fernandez G, Gautron L, Valdivia LS. The controversial role of the vagus nerve in mediating ghrelin´s actions: gut feelings and beyond. IBRO Neuroscience Reports. 2022 Mar DOI: 10.1016/j.ibneur.2022.03.003

89 Craig ADB. Forebrain emotional asymmetry: a neuroanatomical basis? Trends Cogn Sci (Regul Ed). 2005 Dec;9(12):566–71.

90 Bakker R, Tiesinga P, Kötter R. The Scalable Brain Atlas: Instant Web-Based Access to Public Brain Atlases and Related Content. Neuroinformatics. 2015 Jul;13(3):353–66.

FIGURE LEGENDS

Fig. 1. Overall experimental design. The figure summarizes the experimental design used in the current study. The pink region represents the expected time-course of plasma ghrelin after subcutaneous injection, indicated by the blue arrow, common to the three experimental conditions (E1, E2, E3). Plasma ghrelin is expected to remain low at basal levels of fed mice in the case of vehicle injection. The green regions represent the expected time course of ^{18}F-FDG uptake after its intraperitoneal injection, marked by a red solid line and arrow for each experimental condition, followed by a red dashed line and a yellow box representing the onset and duration of the inhalatory anesthesia, and a gray box to indicate the acquisition period.

Fig. 2. Differential ^{18}F-FDG uptake during the 0–10 minutes time windows after ghrelin treatment (E1). Panel **A** shows ^{18}F-FDG PET coronal t-static images for the comparison of ghrelin vs. vehicle treated mice, co-registered and overlaid with a serial two photon tomography average mouse template. The maps are colored using a dual black–to–orange and black–to–blue color lookup Fig. 5 (shown on the left) to indicate increased and decreased ^{18}F-FDG uptake, respectively, starting from the significance threshold of $p < 0.05$. Panel **B** show three volumetric views of the regions with significant changes in ^{18}F-FDG uptake. From left to right, a front-top-left, front-top, and front-top-right views are shown. A saturated orange or blue color indicate increased or decreased uptake, respectively. These views were generated using Fiji [44] and the Scalable Brain Atlas [90] Composer. Scale bar: 4 mm divided into 1 mm segments.

Fig. 3. Differential ^{18}F-FDG uptake during the 10–20 minutes time windows after ghrelin treatment (E1). Panel **A** shows ^{18}F-FDG PET coronal t-statistic images for the comparison of ghrelin vs. vehicle treated mice, co-registered and overlaid with a serial two photon tomography average mouse template. The maps are colored using a dual black–to–orange and black–to–blue color lookup Fig. 5 (shown on the left) to indicate increased and decreased ^{18}F-FDG uptake, respectively, starting from the significance threshold of $p < 0.05$. Panel **B** show three volumetric views of the regions with significant changes in ^{18}F-FDG

uptake. From left to right, a front-top-left, front-top, and front-top-right views are shown. A saturated orange or blue color indicate increased or decreased uptake, respectively. These views were generated using Fiji [44] and the Scalable Brain Atlas [90] Composer. Scale bar: 4 mm divided into 1 mm segments.

Fig. 4. Differential ^{18}F-FDG uptake during the 20–30 minutes time windows after ghrelin treatment (E3). Panel **A** shows ^{18}F-FDG PET coronal t-static images for the comparison of ghrelin vs. vehicle treated mice, co-registered and overlaid with a serial two photon tomography average mouse template. The maps are colored using a dual black–to–orange and black–to–blue color lookup Fig. 5 (shown on the left) to indicate increased and decreased ^{18}F-FDG uptake, respectively, starting from the significance threshold of $p < 0.05$. Panel **B** show three volumetric views of the regions with significant changes in ^{18}F-FDG uptake. From left to right, a front-top-left, front-top, and front-top-right views are shown. A saturated orange or blue color indicate increased or decreased uptake, respectively. These views were generated using Fiji [44] and the Scalable Brain Atlas [90] Composer. Scale bar: 4 mm divided into 1 mm segments.

Fig. 5. Summary of brain areas with significant change of ^{18}F-FDG uptake in each experimental condition. The figure summarizes the brain areas where a significant change of ^{18}F-FDG uptake was observed for each experimental condition (E1, E2, E3). The references for the colors and side of the signals are shown as an independent diagram at the bottom right. Specifically, orange indicates increased ^{18}F-FDG uptake, blue indicates decreased ^{18}F-FDG uptake, and gray indicates unchanged ^{18}F-FDG uptake.

Fig. 6. Localization of fluorescent signal in mice systemically-injected with Fr-ghrelin. Panels **A-F** show representative microphotographs of the Fr-ghrelin signal observed in the in the CP (**A**), SFO (**B**), SCO (**C**), OVLT (**D**), AP (**E**) and hippocampus (**F**) of mice that were SC-injected with Fr-ghrelin. Panels **G-H** show and the right and left ARH of vehicle (**G**) and Fr-ghrelin (**H**) treated mice, respectively. Each panel shows a high magnification image of the areas marked in the low magnification image. Cell nuclei were labeled with Hoechst. Arrows point at Fr-ghrelin signal. Panel **I** shows the quantification of fluorescent signal in the right and left ARH of mice that were SC-injected with Fr-ghrelin. pc: posterior commissure; CA1, CA2, CA3: hippocampal fields 1, 2 and 3; DG: dentate gyrus. Scale bars, 100 µm (low magnification, 10x objective) and 10 µm (high magnification, 40x objective).

Fig. 7. Induction of c-Fos in mice systemically-injected with ghrelin. Panel **A-B** show a representative microphotograph of c-Fos immunolabeling in the right and left ARH of mice that were SC-injected with vehicle (**A**) or ghrelin (**B**). Panel **C** shows the quantification of the number of c-Fos-IR cells in the right and left ARH of mice that were SC-injected with ghrelin. Scale bars, 100 µm (low magnification, 10x objective).

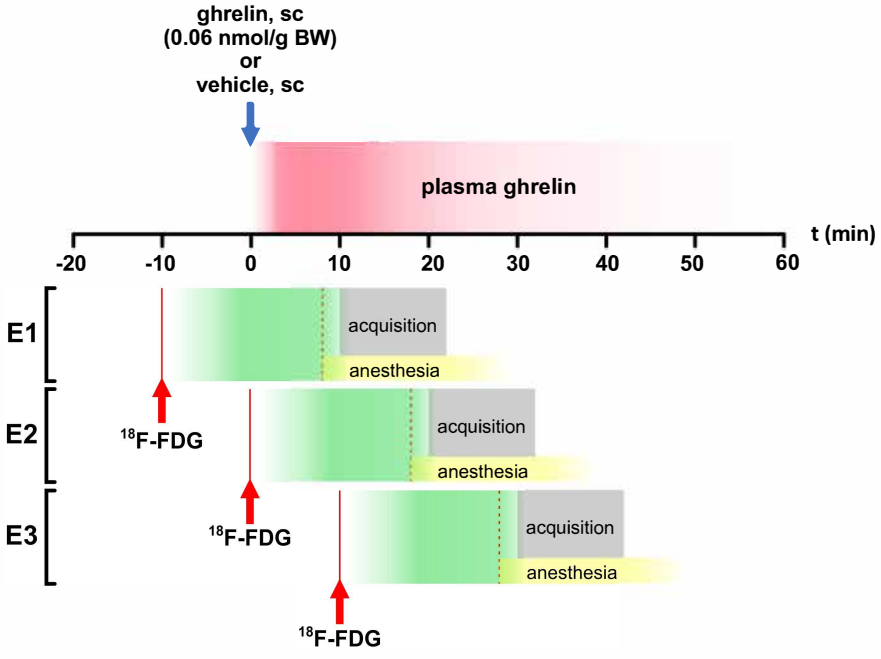
ghrelin, sc
(0.06 nmol/g BW)
or
vehicle, sc
plasma ghrelin
t (min)
-20
-10
0
10
20
30
40
50
60
E1
acquisition
anesthesia
E2
18F-FDG
acquisition
anesthesia
E3
18F-FDG
acquisition
anesthesia
18F-FDG

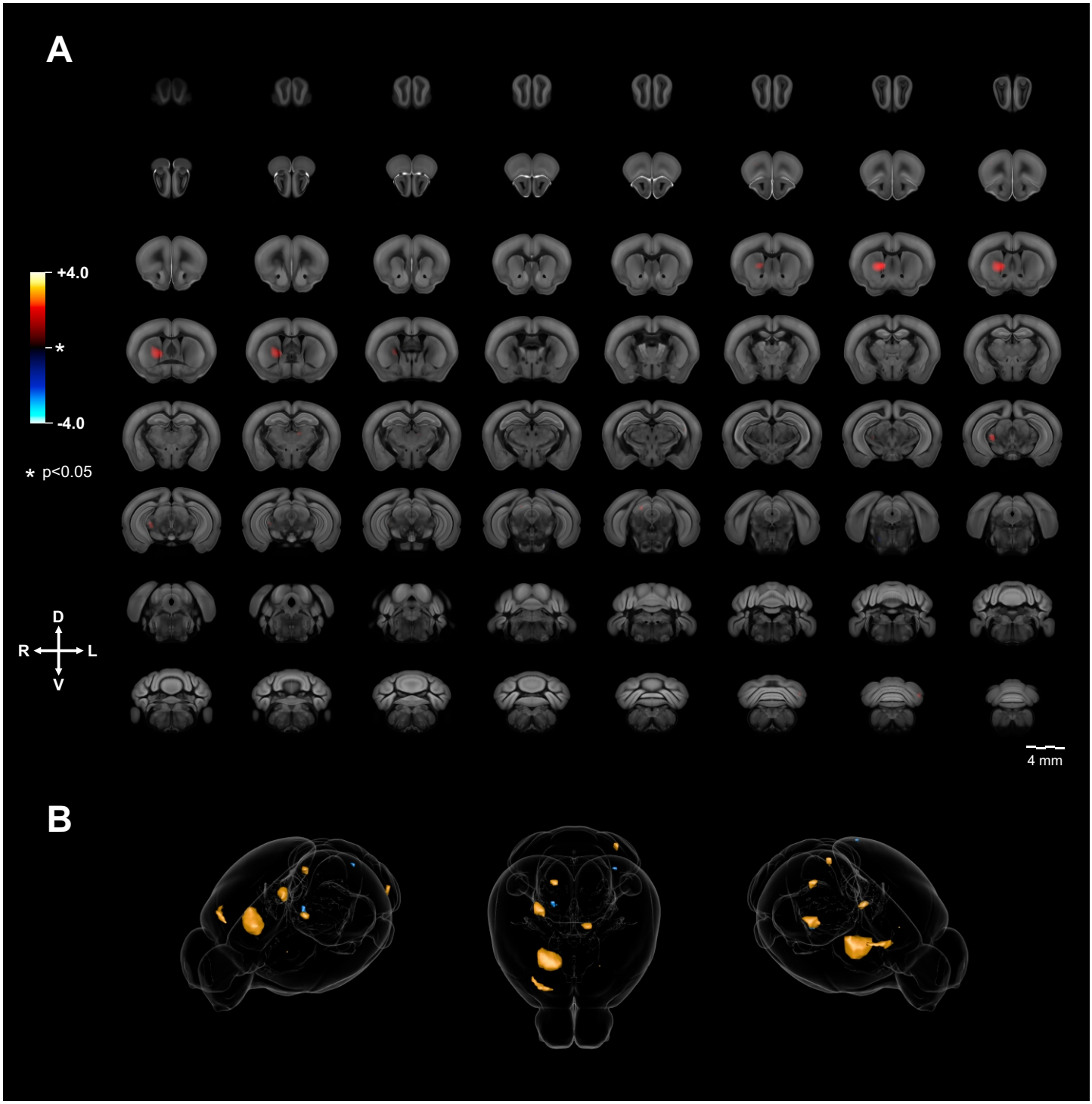
A
+4.0
*
-4.0
* p<0.05
D
R
L
V
4 mm
B

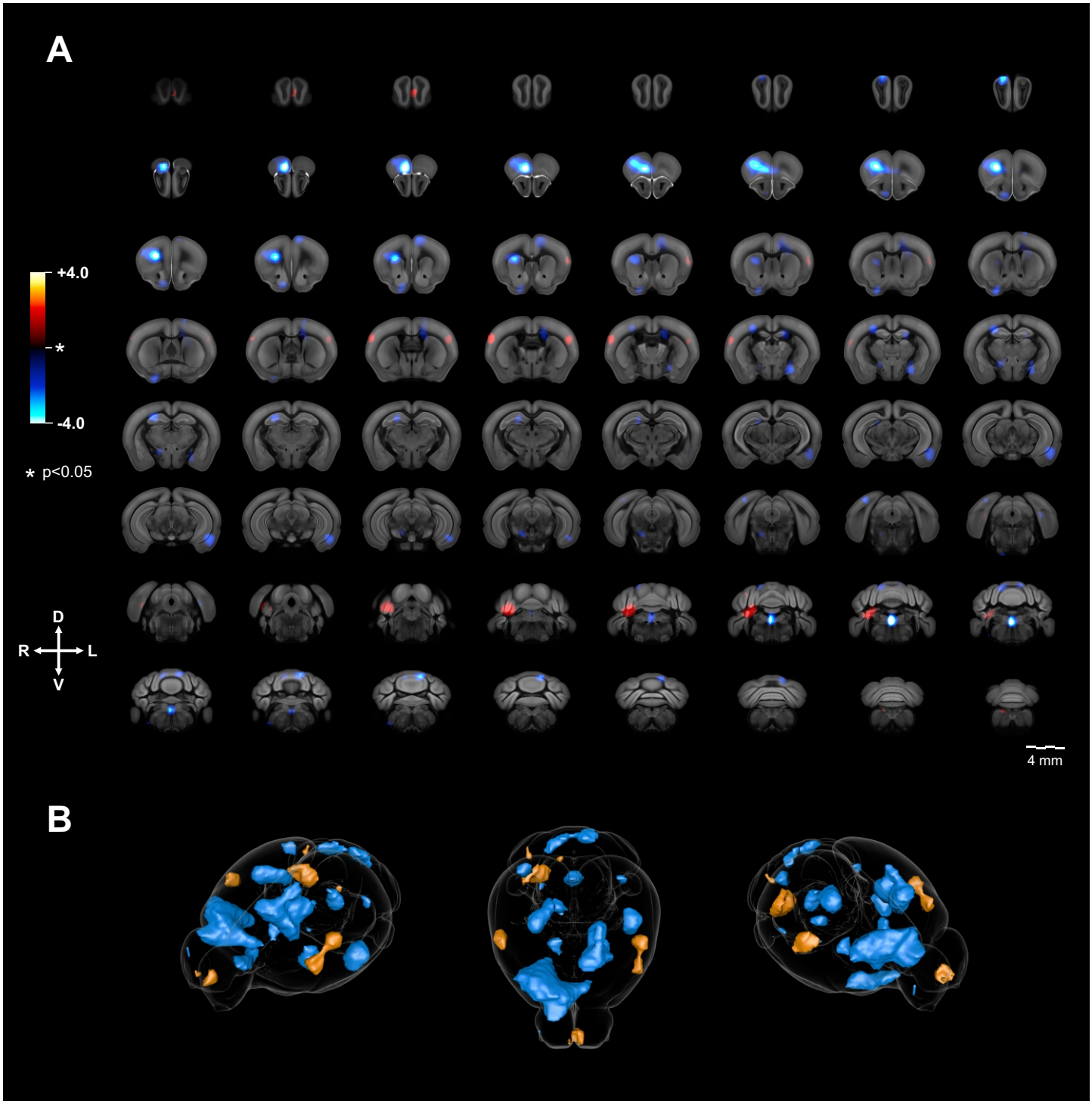
A
+4.0
*
-4.0
* p<0.05
D
R
L
V
4 mm
B

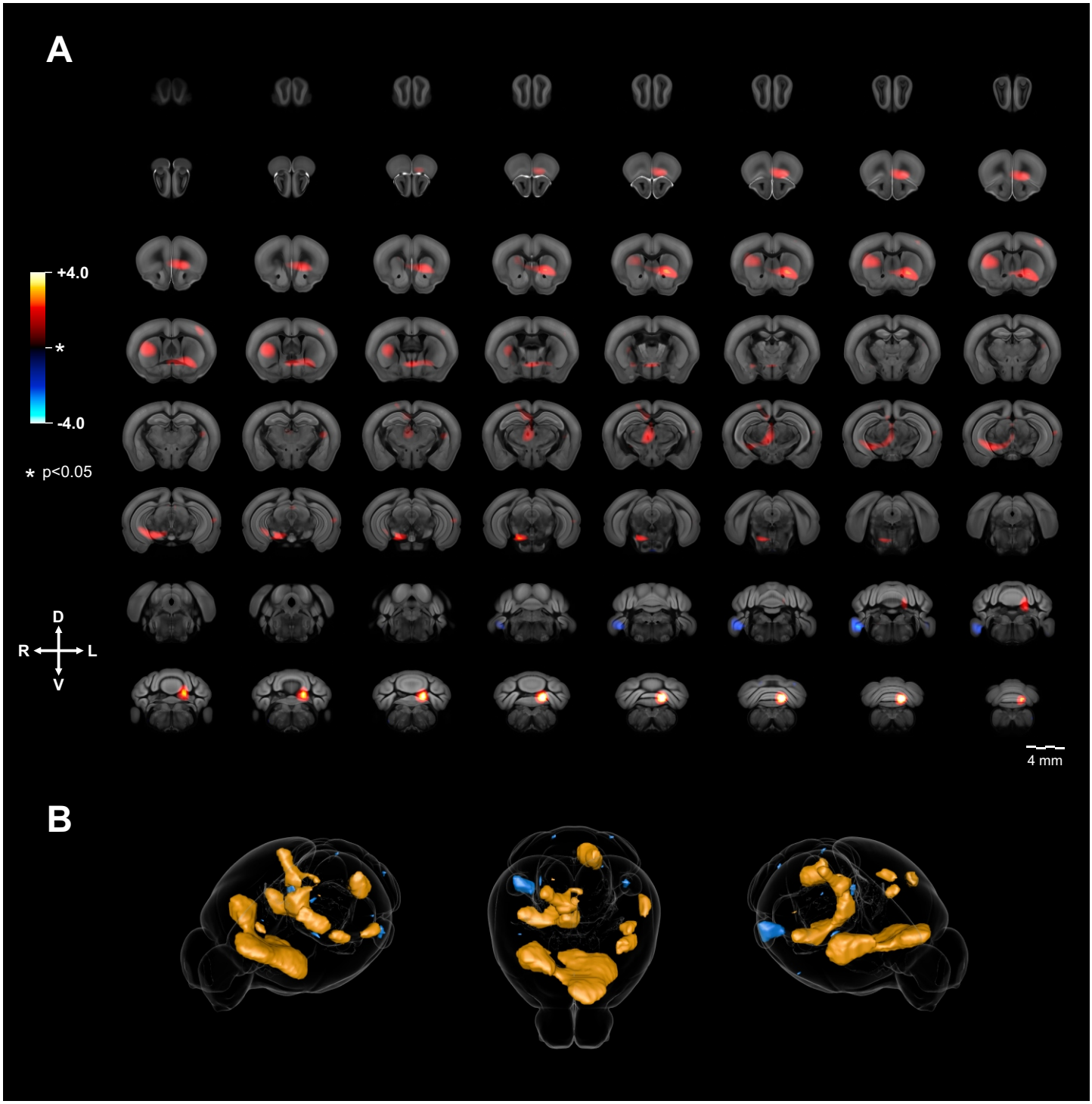
A
+4.0
*
-4.0
* p<0.05
D
R
L
V
4 mm
B

Region	Structure name	E1	E2	E3
Isocortex	Frontal pole, cerebral cortex			
	Primary motor area			
	Secondary motor area			
	Primary somatosensory area, nose			
	Primary somatosensory area, lower limb			
	Primary somatosensory area, mouth			
	Primary somatosensory area, upper limb			
	Primary somatosensory area, unassigned			
	Supplemental somatosensory area			
	Ventral auditory area			
	Anteromedial visual area			
	Primary visual area			
	Anterior cingulate area, dorsal part			
	Anterior cingulate area, ventral part			
	Prelimbic area			
	Infralimbic area			
	Orbital area, lateral part			
	Orbital area, medial part			
	Orbital area, ventrolateral part			
	Agranular insular area, dorsal part			
	Retrosplenial area, lateral agranular part			
	Retrosplenial area, ventral part			
	Anterior area			
	Temporal association areas			
Olfactory areas	Main olfactory bulb			
	Accessory olfactory bulb			
	Anterior olfactory nucleus			
	Taenia tecta, dorsal part			
	Taenia tecta, ventral part			
	Dorsal peduncular area			
	Piriform area			
	Postpiriform transition area			
Hippocampal region	Field CA1			
	Field CA3			
	Dentate gyrus, molecular layer			
	Dentate gyrus, granule cell layer			
Retrohippocampal region	Entorhinal area, lateral part, layer 3			
	Entorhinal area, lateral part, layer 5			
	Entorhinal area, lateral part, layer 6a			
	Parasubiculum			
	Subiculum			
Cortical subplate	Endopiriform nucleus, dorsal part			
	Endopiriform nucleus, ventral part			
	Basolateral amygdalar nucleus, post. part			
Striatum	Caudoputamen			
	Nucleus accumbens			
	Olfactory tubercle			
	Lateral septal nucleus, rostral part			
	Lateral septal nucleus, ventral part			
	Striatum-like amygdalar nuclei			
Pallidum	Globus pallidus, external segment			
	Globus pallidus, internal segment			
	Substantia innominata			
	Magnocellular nucleus			
	Medial septal nucleus			
	Bed nuclei of the stria terminalis			

Region	Structure name	E1	E2	E3
Thalamus	Thalamus, sensory-motor cortex related			
	Medial group of the dorsal thalamus			
	Midline group of the dorsal thalamus			
	Intralaminar nuclei of the dorsal thalamus			
	Medial habenula			
	Lateral habenula			
Hypothalamus	Periventricular zone			
	Hypothalamic lateral zone			
Midbrain	Inferior colliculus, external nucleus			
	Substantia nigra, reticular part			
	Ventral tegmental area			
	Midbrain reticular nucleus			
	Superior colliculus, motor related			
	Periaqueductal gray			
	Pretectal region			
	Midbrain, behavioral state related			
Pons	Pontine central gray			
	Pons, behavioral state related			
Medulla	Medulla, sensory related			
	Paragigantocellular reticular nucleus			
	Perihypoglossal nuclei			
	Medial vestibular nucleus			
Cerebellum	Lobule III			
	Lobules IV-V			
	Declive (VI)			
	Pyramus (VIII)			
	Uvula (IX)			
	Nodulus (X)			
	Simple lobule			
	Copula pyramidis			
	Paraflocculus			
	Flocculus			
	Cerebellar nuclei			

	left decrease	left n/s	left increase
right decrease			
right n/s			
right increase			

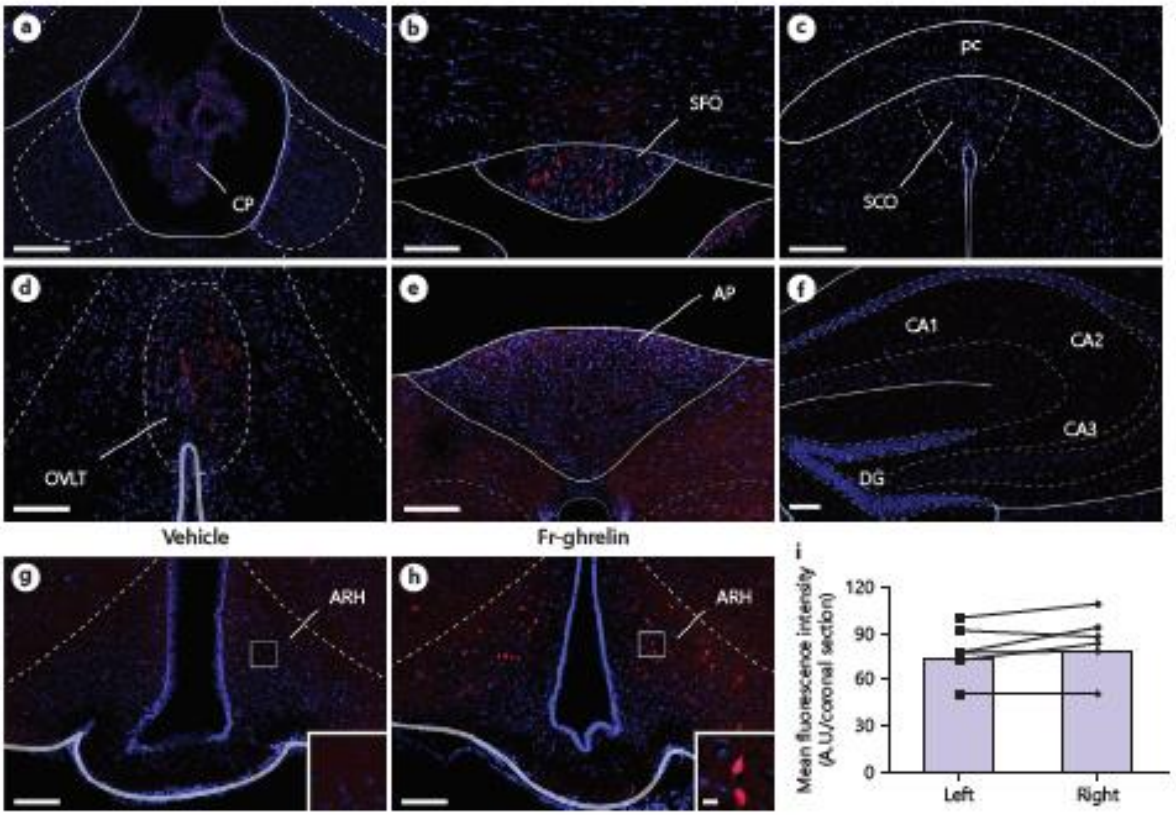
a
CP
b
SFO
c
PC
SCO
d
OVLT
e
AP
f
CA1
CA2
CA3
DG
Vehicle
Fr-ghrelin
g
ARH
h
ARH
i
Mean fluorescence intensity (A.U./coronal section)
120
90
60
30
0
Left
Right

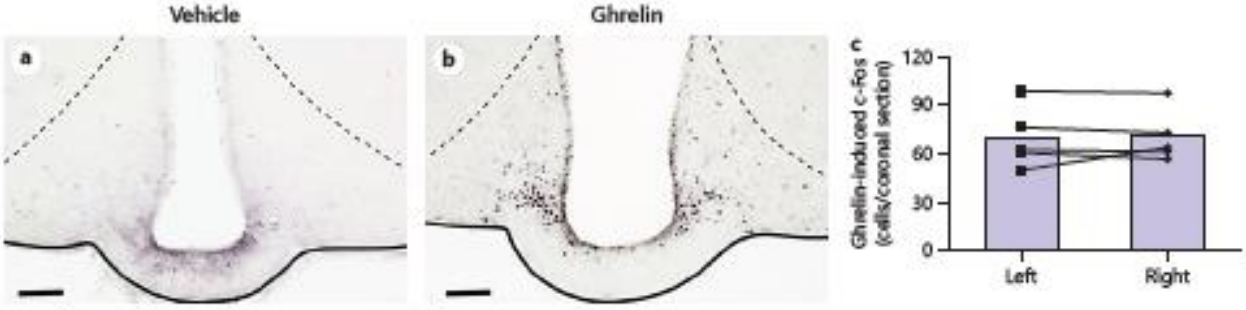
Vehicle
Ghrelin
a
b
c
Ghrelin-induced c-Fos
(cells/coronal section)
120
90
60
30
0
Left
Right